Supporting Information

Directing Assembly and Disassembly of 2D MoS_2 Nanosheets with DNA for Drug Delivery

*Bang Lin Li,[1,#] Magdiel I. Setyawati,[1,#] Linye Chen,[1] Jianping Xie,[1] Katsuhiko Ariga,[2] Chwee-Teck Lim,[3,4,5,6] Slaven Garaj,[3,4,7] and David Tai Leong[1,]***

[1]Department of Chemical and Biomolecular Engineering, National University of Singapore, Singapore 117585, Singapore.

[2]World Premier International (WPI) Research for Materials Nanoarchitectonics (MANA), National Insitute for Materials Science (NIMS), 1-1 Namiki, Tsukuba 305-0044, Japan.

[3]Department of Biomedical Engineering, National University of Singapore, Singapore 117575, Singapore.

[4]Centre for Advanced 2D Materials, Graphene Research Centre, National University of Singapore, Singapore 117546, Singapore.

[5]Mechanobiology Institute, National University of Singapore, Singapore 117411, Singapore.

[6]NUS Graduate School for Integrative Sciences and Engineering, National University of Singapore, Singapore 117456, Singapore.

[7]Department of Physics, National University of Singapore, Singapore 117542, Singapore.

[#]These authors contribute equally to this work.

*Correspondence and requests for materials should be addressed to D. T. L. (cheltwd@nus.edu.sg)

Experimental Sections

1. Materials. Molybdenum(IV) sulfide (MoS_2 crystalline powder, < 2 μm, 99%), sodium cholate (98%), SYBR Green I, 3D micro-mold and Doxorubicin hydrochloride (Dox) were purchased from Sigma-Aldrich Co. (USA). All DNA oligonucleotides, shown in Table S1, were obtained from Sangon, Inc. (Shanghai, China). Breast cancer cells, MDA-MB-468 and MCF-7, were purchased from ATCC, USA. The ATP assay kit was obtained from Abcam Co., Singapore. SYTOX Green, Alexa Fluor 488 conjugated Annexin V, and LysoTracker Green dyes were obtained from Life Technologies, USA. Agarose and 10 × Tris-acetate-EDTA (TAE) buffer solutions (100 mg mL^{-1} NaCl and 10 mg mL^{-1} MgCl) were purchased from First Base, Singapore. The enzyme DNase was obtained from Thermo Fisher Scientific Co., USA.

2. Instruments. Bath sonicator (Thermo Fisher, USA) and centrifugator (Hitachi, Japan) were used for the sonication and separation, respectively. The DNA was hybridized using thermal cycler (Bio-Rad, USA) and subsequently separated with polyacrylamide gel electrophoresis (PAGE) (Bio-Rad, USA). Cell death was determined with Tali Image based cytometer (Life Technologies, USA). The fluorescence intensities and absorbance detections were conducted using microplate reader (BioTek H4FM, USA). Atomic force microscrope (Bruker, Germany) was used for the thickness measurements. Zetasizer (Malvern, UK) was utilized for detections of Z-average diameters and zeta potential values. Fluorescence imaging were taken with inverted fluorescence microscope (Leica DMI6000, Germany), while the phase contrast images were captured by inverted microscope (Olympus-CX41, Japan).

3. Exfoliation of Bulk MoS_2 Powders. MoS_2-NS was obtained through liquid phase exfoliation of bulk MoS_2 powders in sodium cholate aqueous solution.[S1] First of all, a portion of 200 mL aqueous mixture solution, containing 5 mg mL^{-1} MoS_2 powders and 1.5 mg mL^{-1} sodium cholate,

was sonicated for 20 h, where a black dispersion was obtained. Subsequently, the dispersion was centrifuged at 3 000 rpm for 30 min and a yellow-green supernatant containing sodium cholate and exfoliated MoS_2-NS was collected. In order to remove the sodium cholate, the yellow-green mixture was centrifuged (10 000 rpm, 30 min) and MoS_2-NS sediments were collected. The washing process was conducted through re-dispersing the collected MoS_2-NS in ultrapure water *via* sonication, and the regenerated dispersion was centrifuged (10 000 rpm, 30 min), followed by the collection of sediments. The washing process was then repeated two times to thoroughly remove sodium cholate absorbed on MoS_2-NS. Ultimately, the sediments were well-dispersed in ultrapure water to obtain uniform MoS_2-NS aqueous dispersions. In order to confirm a repeatable experiment result, MoS_2-NS stock solutions should be used after sonication for 5 min.

4. Functionalization of Thiol-Labelled DNA on MoS_2-NS. A portion of thiol-labelled DNA (DNA-SH) solution was added into MoS_2-NS aqueous dispersion, which was then diluted to 1 × TAE buffer solution containing 200 μg mL^{-1} MoS_2-NS and 1 μM DNA-SH. Subsequently, the mixed solution was sonicated in bath sonicator for 10 seconds and then incubated at room temperature (25 ℃) for 5 h, resulting with the attachment of thiol groups on MoS_2-NS. In order to remove the unattached DNA oligonucleotides, the resultant MoS_2-NS solution was centrifugated at 10 000 rpm for 30 min to allow nanosheets to settle down and the supernatant to be separated. The concentration of unattached DNA in resultant supernatant was detected based on SYBR Green I assay. Ultimately, the sediments of DNA-SH functionalized MoS_2-NS were collected and then re-dispersed into ultrapure water or culture medium for further research.

5. Absorbance Measurements of MoS_2-NS Dispersions. According to Beer-Lambert Law, Absorbance of MoS_2-NS and DNA/MoS_2-NS aqueous dispersions corresponds to the concentrations of nanosheets in the supernatant (top 2/3 of samples). This allows the

determination of dispersed and aggregated state of MoS_2-NS and DNA/MoS_2-NS in different conditions.[S1] In order to assess the dispersed properties of MoS_2-NS in the absence and presence of DNA-SH, absorbance of the resultant supernatant at wavelength of 605 nm was detected after different standing times. MoS_2-NS before and after the treatments of pure DNA and thiol-labelled DNA were dispersed in high-concentration salts solutions and the absorbance of supernatant for each sample was recorded in the beginning (A_{0h}) and after 12 hours (A_{12h}), respectively. The increase of A_{12h}/A_{0h} value corresponds to the dispersion improvement of nanosheets.

6. SYBR Green I Assay. In order to calculate the amount of DNA duplex attached on MoS_2-NS surface, SYBR Green I assay was introduced. After MoS_2-NS dispersions were incubated with different kinds of DNA duplex (unmodified D1, D1-S-S-D1, and D1), the resultant composites were centrifuged (10 000 rpm, 30 min). Apparently, the supernatants were colorless and all DNA/MoS_2-NS composites were totally deposited. Subsequently, 1 × SYBR Green I solution was added into the collected supernatant. Of significance, SYBR Green I dye combined with the remaining duplex in the supernatant, leading to the obvious enhancement of fluorescence intensity (Ex/Em=485/525 nm). The fluorescence intensity of SYBR Green I in remaining supernatant was recorded for calculating the amount of duplex functionalized on MoS_2-NS.

7. Dox Loading of DNA Duplex. Equimolar P1 and ATP aptamer were mixed and hybridized for 30 min in 1× TAE buffer solution to form stable thiolated duplex structure (D1). Dox solution was then added in the D1 solution, making the concentration of Dox was twice than that of D1. Subsequently, the Dox and DNA mixture solution was incubated at 37 ℃ for 1 hour and the Dox molecules were successfully intercalated into the inner duplex structure, resulting in the complete quenching of fluorescence. In order to calculate the loading efficacy of D2, the

fluorescence intensities of Dox solutions in the absence and presence of D2 were recorded (Ex/Em=480/595 nm).

8. Dox Loading of D1/MoS_2-NS. After the formation of D1 functionalized MoS_2-NS (D1/MoS_2-NS), Dox solution was added. The mixed solution was incubated and gently shaken in a shaker at 37 ℃ for 1 h with stirring at 300 rpm, resulting in both intercalation and absorption of Dox molecules on D1/MoS_2-NS to form Dox/D1/MoS_2-NS. The fluorescence intensities of Dox before and after incubation with D1/MoS_2-NS were recorded (Ex/Em=480/595 nm). For calculating the loading efficacy, the mixture was centrifuged at 12 000 rpm for 30 min, making Dox/D1/MoS_2-NS deposited. The absorbance of collected supernatant at wavelength of 500 nm was measured to calculate the remaining Dox concentration. Similarly, the drug loading capacity of MoS_2-NS was determined following the above mentioned process with the pure MoS_2-NS instead of D1/MoS_2-NS.

9. *In vitro* ATP-Induced Dox Release. The as-prepared Dox/D1/MoS_2-NS was incubated with different concentrations of ATP in 1 × TAE buffer solution, and gently shaken at 37 ℃ in a shaker at 100 rpm for 30 min. The resultant solution was centrifugated at 15 000 rpm for 10 min and the supernatant containing Dox was collected. In our protocol, the Dox in supernatant was released from platform of Dox-composites in the presence of ATP. Ultimately, the fluorescence intensity of Dox released was detected at 595 nm with an excitation wavelength of 480 nm using a microplate reader. Similarly, the drugs release experiments of Dox/D1 and Dox/MoS_2-NS were conducted following the above mentioned process with Dox/D1 and Dox/MoS_2-NS instead of Dox/D1/MoS_2-NS, respectively.

10. Cell Culture. Dulbecco's Modified Eagle Medium (DMEM) supplemented with 10% fetal bovine serum (FBS) and 1% Penicillin/Streptomycin cocktail, hereby denoted as cell culture

medium, was used to grow the MDA-MB-468 and MCF-7 cells. The cells were grown in standard culture condition (37 ℃, 5% CO_2, 95% relative humidity) and were sub-cultured when they reach 90% confluence.

11. Intracellular ATP Assay. The content of ATP in the cells was detected by the ATP assay kit. MDA-MB-468 cells (1×10^6 cells/cm^2) treated with three different conditions were lysed with 100 μL ice-cold ATP assay buffer and then centrifuged at 15 000 ×g for 2 min to pellet insoluble materials. After centrifugation, the supernatant (50 μL) was collected and subsequently diluted using ATP assay buffer twice. The fluorometric detection of the final solution (100 μL) was conducted using the microplate reader (Ex/Em=537/587 nm).

12. Intracellular Dox Release. MDA-MB-468 cells (4×10^4 cells/cm^2) were seeded in 24-well plates for 24 h. Afterwards, the cells were treated with different Dox-composites for 60 min. The treatment medium was removed and the cells were washed three times with 1 × phosphate buffer solution (PBS, pH 7.4). The cells then were further incubated in in Dox-free medium for 30 min to allow the release of Dox in cells. The Dox content released was determined by measuring the intensity of fluorescence using the microplate reader (Ex/Em=480/595 nm). In order to prove the role of ATP in drug release of our developed nanocarriers, intracellular ATP-rich and ATP-poor conditions were provided and the cell culture medium with supplied with high-concentration (4.5 g L^{-1}) and low-concentration glucose (1.0 g L^{-1}) solutions, respectively.

13. *In vitro* Cytotoxicity of Dox/D1/MoS_2-NS. MDA-MB-231 and MCF-7 cells (4×10^4 cells/cm^2) were seeded in 24-well plates. After culture for 24 h, the cells were treated with Dox/D1/MoS_2-NS for 24 h. Following that, the treated cells were collected and stained with SYTOX Green and the cell death was assessed with Tali image based cytometer. Comparative

cytotoxicity experiments of D1/MoS_2-NS, Dox only, Dox/D1, and Dox/MoS_2-NS were also carried out by maintaining the same Dox concentration throughout the treatment regime.

14. Formation of Layer-by-Layer Dox/D2/MoS_2-NS. Thiolated ssDNA (P2) functionalized MoS_2-NS (P2/MoS_2-NS) were mixed with another thiolated ssDNA (P3) functionalized MoS_2-NS (P3/MoS_2-NS) at the ratio of 1:1 in the 1 × TAE buffer solution, followed by the addition of ATP aptamer and Dox solution. The mixed solution was incubated and gently shaken in a shaker at 37 ℃ for 12 h with stirring at 300 rpm to from layer-by-layer Dox/D2/MoS_2-NS (LbL-Dox/D2/MoS_2-NS) *via* ATP aptamer induced interlayer assembly. To evaluate the ATP-responsive dissociation of LbL-Dox/D2/MoS_2-NS, the as-prepared composites were incubated with different concentrations of ATP at 37 ℃ for 2 h. Control experiments were conducted using non-complementary DNA in lieu of ATP aptamer.

15. Inhibition of Enzymatic Digestion. DNase I was used to study the enhanced protective effect of single-layer Dox/D1/MoS_2-NS and LbL-Dox/D2/MoS_2-NS against enzymatic digestion. First of all, Dox molecules were loaded on different drug carriers (D1, D1/MoS_2-NS, LbL-D2/MoS_2-NS), whereas the concentrations of duplex structure in different carriers are fixed and saturated. Subsequently, Dox-loading carriers were treated with 5 U/mL of human deoxyribonuclease (DNase) I in 1 × enzyme buffer solution at 37 ℃ for different incubation times ranging from 10, 20, 30, 40, 50, and 60 min. Following enzyme treatments, those samples were centrifugated at 15 000 rpm for 10 min and the supernatant containing free Dox was collected. The fluorescence of supernatant was detected using microplate reader (Ex/Em=480/595 nm). In this protocol, the fluorescence of samples before the treatment of enzyme was name as F_0, whereas those treated with DNase I with different incubation times

were labelled as F_t. ΔF, defined as the intensity changes from F_0 to F_t, indicates the release of Dox from different kinds of Dox-loading carriers.

16. 3D Cell Culture. Tumor spheroids were formed with the help of non-adherent agarose micro-molds as previously described.[S2] Briefly, micro-molds were formed by casting 2% agarose solution and let it to solidify. Prior use, the micro-molds were placed in 24-wells plate, sterilized with UV irradiation for 30 min, and soaked with complete DMEM overnight. In each of the micro mold, 2×10^5 MDA-MB-468 cells were added and left to settle and aggregate for 24 h to form the desired tumor spheroids. For acute treatment, the tumor spheroids were flushed out from the micro-mold and moved to a new well which were coated with a flat layer of 2% non-adherent agarose. Thereafter, the tumor spheroids were treated with different Dox carriers (as depicted in Table S2) for 24 and 48 h. At the end of treatment time, the tumor spheroids were collected, washed, and re-dispersed with the help of trypsin-EDTA. The dispersed cells then were collected and stained with Alexa Fluor 488 conjugated Annexin V (1:20). The apoptotic cells then were detected with Tali image based cytometer. TAE buffer (pH 7.4) at the same dilution factor was used as vehicle control. For sub-chronic treatment, the tumor spheroids were directly treated within the agarose micro-molds. The treatment was conducted by introducing the tumor spheroids to 1/10 of the treatment dose depicted in Table S2). The treatment was changed every day over the course of 5 days. To assay the sub-chronic effect of the treatment regime, the bright field images of the tumor spheroids were captured with the Olympus inverted microscope and the size of the tumor spheroids (n = 15) were measured with imageJ software.[S3]

Table S1. DNA name corresponding to the sequence in the content.

Name	Sequence
Unmodified P1	5'-GTGTACCTTCCTCCGCAATACTCCCCCAGGT-3'
P1	SH- 5'-GTGTACCTTCCTCCGCAATACTCCCCCAGGT-3'
P1-S-S-P1	5'-GTGTACCTTCCTCCGCAATACTCCCCCAGGT-3'-S-S-3'-TGGACCCCCTCATAACGCCTCCTTCATGTG-5'
P2	SH-5'-GTGTGTACCTTCCTCCGC-3'
P3	5'-AATACTCCCCCAGGTGTGTGT-3'-SH
ATP aptamer	5'-ACCTGGGGGAGTATTGCGGAGGAAGGT-3'
FAM-ATP aptamer	5'-ACCTGGGGGAGTATTGCGGAGGAAGGT-3'-FAM
Non-cDNA	5'-ATTCTTTTTTACAATACTCCCCCAGGT-3'

Table S2. Dox loading amount of different nanocarriers.

Number	Category	Concentration		
		Duplex (μM)	MoS_2 ($\mu g\ mL^{-1}$)	Dox (μM)
1	Dox/D1[(a)]	1 μM	-	2.0
2	Dox/MoS_2-NS	-	200	2.8
3	Single-layer Dox/D1[(a)]/MoS_2-NS	1 μM	200	4.6
4	LbL-Dox/D2[(b)]/MoS_2-NS	1 μM	400	7.0

[(a)]: D1 was formed *via* hybridization of P1 and ATP aptamer.

[(b)]: D2 was formed *via* hybridization of P2, P3 and ATP aptamer.

FIGURE S1

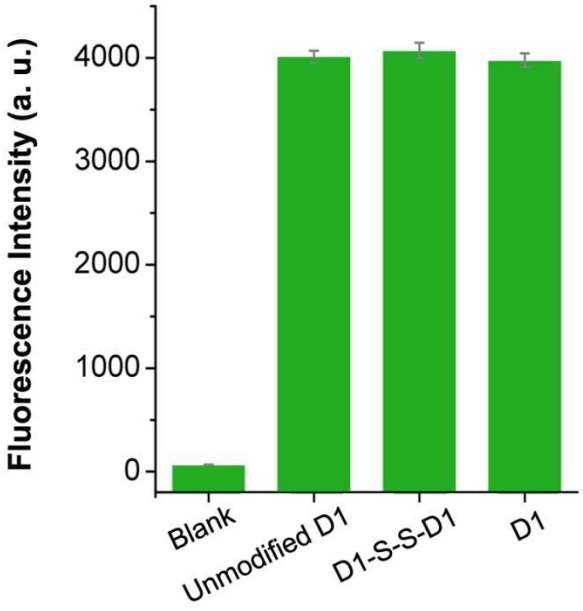

Figure S1. The formations of various DNA duplex structures (unmodified D1, D1-S-S-D1, and D1) were ascertained with SYBR Green I. The fluorescence intensities of SYBR Green I dyes before and after incubation with unmodified D1, D1-S-S-D1, and D1. The duplex structures in those DNA structure are kept in the same concentration of 1 μM.

From Figure S1, it was found that the fluorescence of SYBR Green I significantly increased in the presence of DNA duplex. As SBYR Green fluoresces when it intercalates on the DNA double helix structure, this increase in the fluorescence signals signified successful formation of the DNA duplex. This increase, however, was observed to be in the consistent regardless the different thiol group modification on the introduced DNA duplex (unmodified D1, D1-S-S-D1, and D1).

FIGURE S2

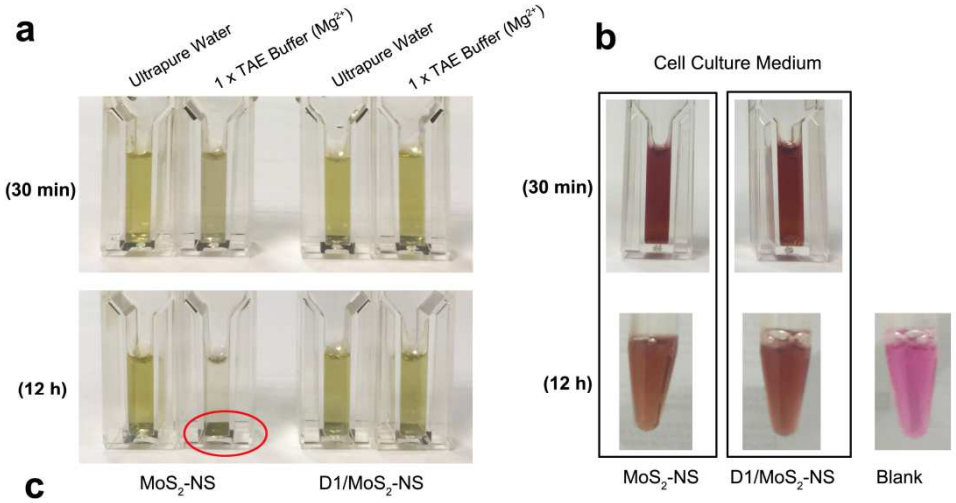

Nanomaterial	Solvent	Z-Average Size (nm)	PDI Number
MoS_2-NS	Ultrapure water	201.8	0.287
	1 x TAE buffer (Mg^{2+})	7153.2*	0.663
	Cell culture medium	253.4	0.275
D1/MoS_2-NS	Ultrapure water	218.2	0.301
	1 x TAE buffer (Mg^{2+})	287.3	0.342
	Cell culture medium	232.1	0.313

Figure S2. Functionalization of DNA facilitates the dispersion of MoS_2-NS. (a) Pictures showing the aggregation of MoS_2-NS in the presence of 1 × TAE buffer solution with different standing times of 30 min and 12 h. (b) Pictures showing the great dispersion of MoS_2-NS and D1/MoS_2-NS in cell culture medium with different standing times of 30 min and 12 h. (c) Z-average sizes of MoS_2-NS and D1/MoS_2-NS in different solvents (ultrapure water, TAE buffer solution, cell culture medium), which were measured by the dynamic light scattering technique.

Figure S2a shows a clear color change of the MoS_2-NS following incubation in the 1 × TAE buffer, in which the color of MoS_2-NS darken within 30 min incubation. Prolonged incubation (up to 12 h) led to the absence of the MoS_2-NS from the supernatant, as evidenced by the sediments at bottom of the cuvette. The phenomenon can be ascribed to the presence of high-concentration positive ions that neutralized the negative charges on the surface of MoS_2-NS and subsequently induced the nanosheets aggregation.[S4] In contrast, the DNA functionalization on the MoS_2-NS prevented the nanosheets from aggregating and keeping them well-dispersed even

in the presence of high-concentration salts. As the formulation ultimately will be introduced to cells, we further investigated the stabilities of these MoS_2-NS and D1/MoS_2-NS in the cell culture medium (Figure S2b). Though the cell culture medium also contains high-concentration of salts, pure MoS_2-NS which carry no DNA protective effect was found to be well-dispersed. This increase of pure MoS_2-NS dispersion could be contributed to the presence of thiol group-containing proteins that were absorbed on MoS_2-NS. This in turn induced the increase on the nanosheets' overall negative charges and prevented them from aggregating in cell culture medium. The aggregation of MoS_2-NS in the presence of salts and stabilities of MoS_2-NS and D1/MoS_2-NS was also evident from the changes in the hydrodynamic size measured *via* dynamic lighting scattering techniques (Figure S2c).

FIGURE S3

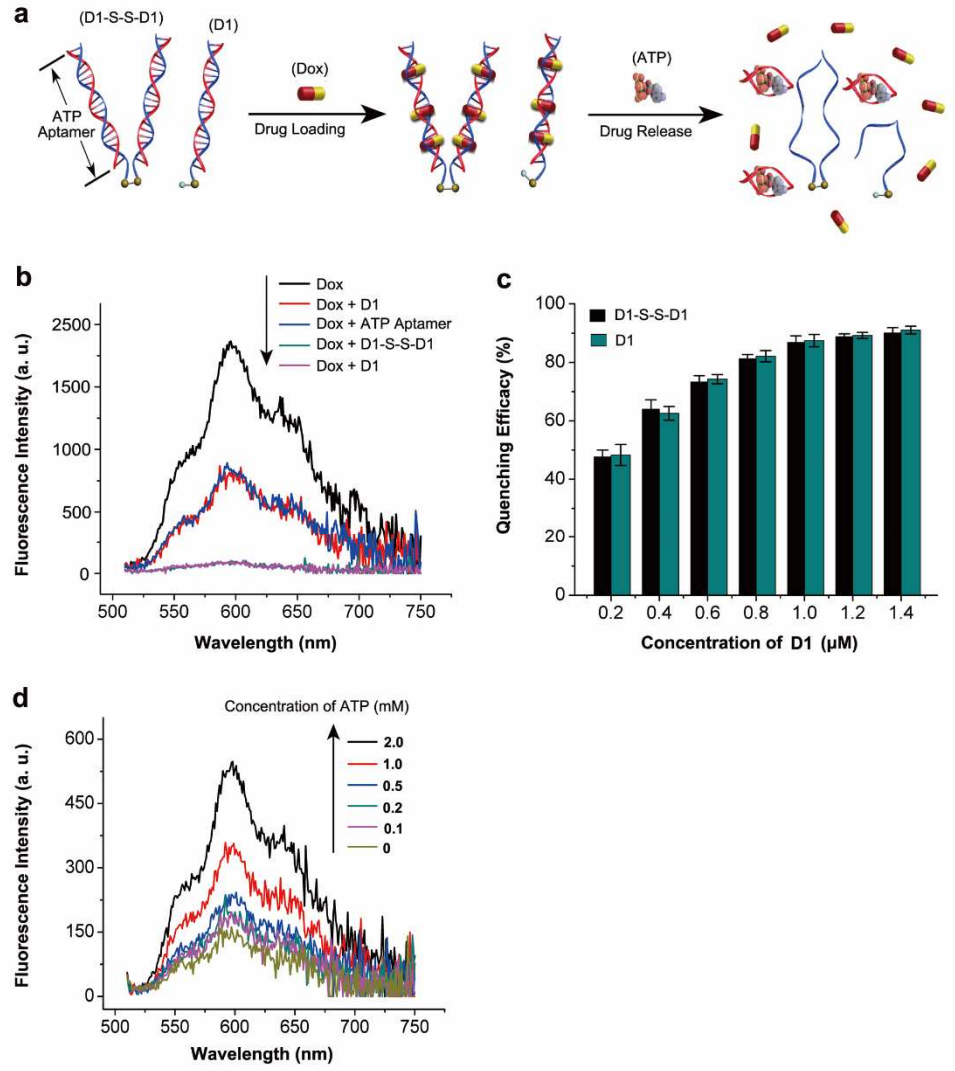

Figure S3. Dox loading of ATP aptamer-based duplex structure. (a) Schematic illustration of Dox-intercalated duplex structure and ATP induced release processes. (b) Fluorescence spectra of Dox in the presence of ssDNA (P1 and ATP aptamer) and dsDNA (D1-S-S-D1 and D1). (c) Quenching efficiency of dsDNA with modifications of thiol group and disulfide bond to Dox. (d) PL spectra of Dox/D1 with the incubation of different concentrations of ATP.

We next investigated the Dox loading efficacy on the thiol modified duplex in addition to its release in response to the ATP induction (Figure S3a). The DNA scaffold formed by hybridization of ATP aptamer and its complementary DNA exhibited Dox loading with a 27-

based pair with GC-rich motif.[S4, S5] The Dox fluorescence signal decreased in the presence of D1 and D1-S-S-D1. This could be attributed to the initiation of Förster resonance energy transfer between Dox molecules that occurred when they intercalated into the duplex structure (Figure S3b). This quenching phenomenon was also observed in single-stranded DNA (ssDNA) groups, i.e. P1 and ATP aptamer, albeit in lesser degree when compared to the duplex DNA structure. This suggests that the ssDNA exhibited much weaker Dox loading efficacy compared to duplex DNA. When a fixed concentration of Dox was incubated with an increasing molar ratio of the duplex DNA, a sequential decrease was detected in the Dox fluorescence intensity (Figure S3c). To investigate the responsiveness of the formed duplex DNA to the stimuli, ATP, we introduced different concentration of ATP to Dox-loaded D1 (Dox/D1) and detected the change in the Dox fluorescence signal. As ATP binds specifically ATP aptamer, it could be expected that in ATP-rich conditions, the ATP would bind to the linearized ATP aptamer in the duplex DNA construct and trigger the ATP aptamer to fold back to their hairpin confirmation. This would result with the duplex DNA structure to be unwound, the Dox to be released from it and subsequently increase the overall Dox fluorescence intensity. Indeed, we observed that the Dox fluorescence signal increase steadily with the more ATP stimuli added into the mixture (Figure S3d). These results confirmed that the thiol group functionalized on the DNA duplex does not influence the loading efficacy of duplex to Dox and its ATP induced release.

FIGURE S4

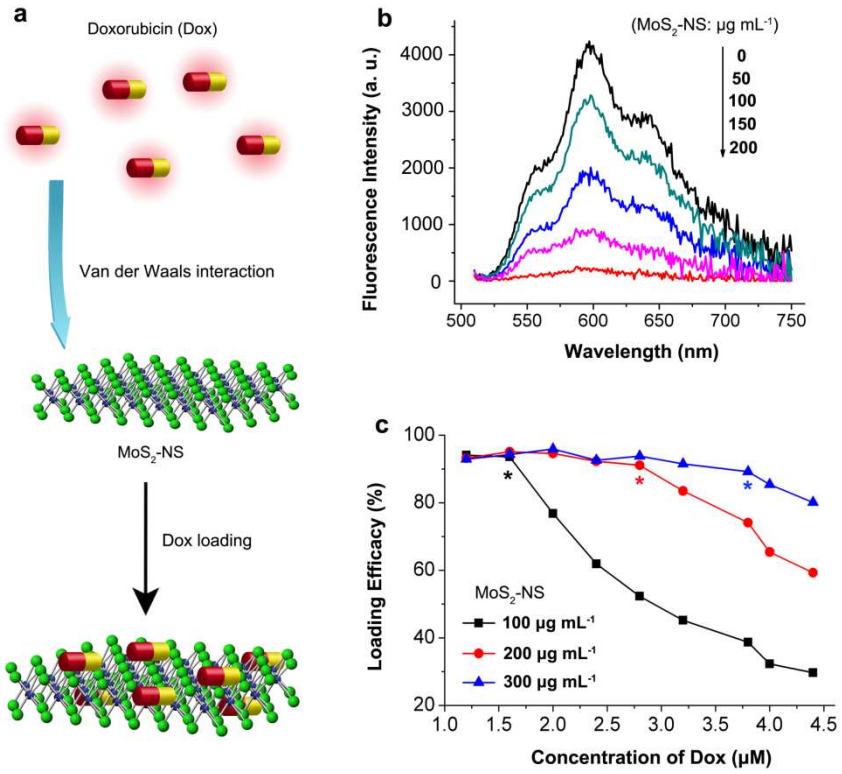

Figure S4. Dox loading of MoS_2-NS. (a) Schematic illustration of Dox loading process on MoS_2-NS. (b) Fluorescence spectra of Dox in the presence of different concentrations of MoS_2-NS. (c) Dose-dependent loading efficiency of MoS_2-NS for Dox.

To determine the Dox loading capacity on pure MoS_2-NS, we utilized the MoS_2-NS obtained from sonication-assisted exfoliation and introduced them with the Dox (Figure S4a). Dox could be incorporated to MoS_2-NS through the surface absorption facilitated by the strong van der Waals force. Because MoS_2-NS has wide absorption at the wavelengths from 400 to 600 nm, this Dox incorporation to MoS_2-NS surface was evident by the significant quenching of the Dox fluorescence signal (Figure S4b). When Dox was introduced at a fixed concentration (3 μM), its fluorescence intensities gradually decreased as the MoS_2-NS concentration increased. The

loading efficacy of different concentrations of MoS_2-NS was calculated, exhibiting the dose-dependent properties (Figure S4c).

FIGURE S5

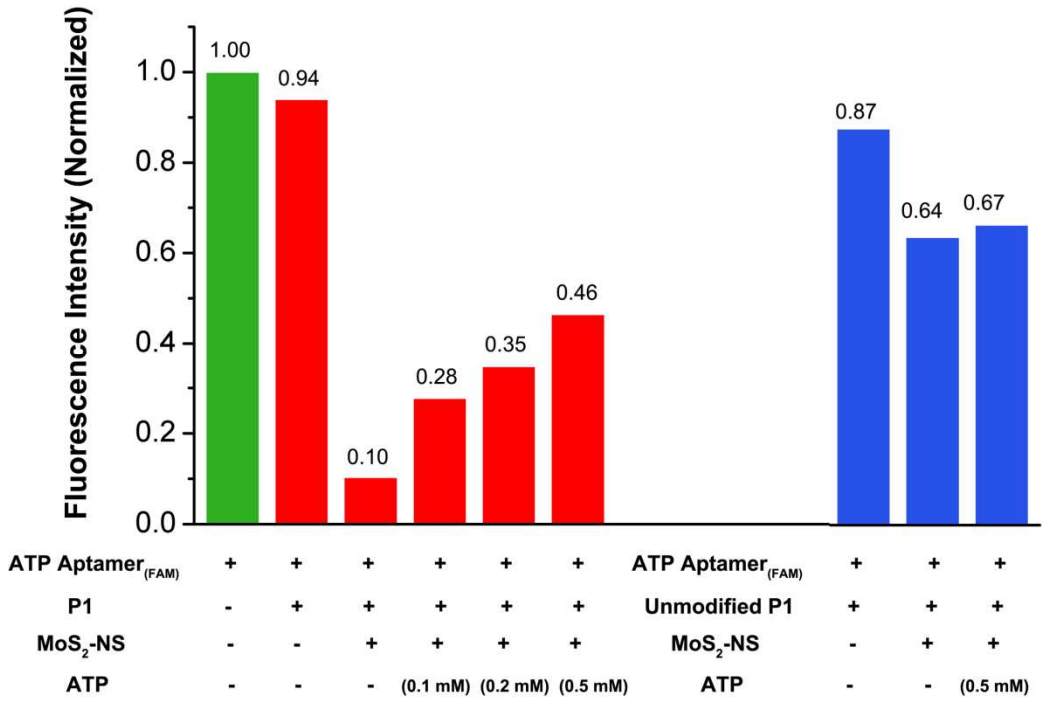

Figure S5. ATP molecules induced the dissociation of duplex on MoS_2-NS platform. Fluorescence intensity of FAM-ATP aptamer after hybridized with its complementary P1 and incubated with MoS_2-NS and different concentrations of ATP.

After hybridization with its complementary ssDNA (P1 or unmodified P1), FAM-ATP aptamer showed a little decrease in its fluorescence intensity. Due to the consequence of thiol group, FAM-D1 got close to the surface of MoS_2-NS and the FAM fluorescence signal was totally quenched (Figure S5). Without the modification of thiol group, a small decrease can be observed, presumably due to unspecific DNA absorption effect onto MoS_2-NS.

FIGURE S6

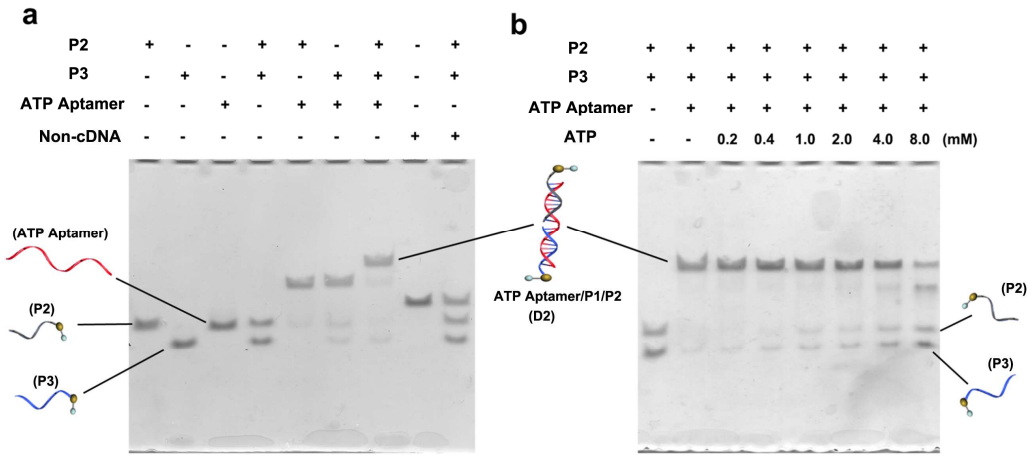

Figure S6. DNA hybridization and ATP-induced dissociation of duplex. (a) Electrophoresis image of DNA hybridization using non-denaturing 12.5% PAGE gel. (b) Electrophoresis image of duplex structure (ATP aptamer/P2/P3) before and after incubation with different concentrations of ATP. DNA structures were separated in 1 × TBE buffer and were visualized following Stains-All staining process.

As shown in Figure S6a, ATP aptamer can hybridize with thiolated P2 and P3 forming duplex (D2). In contrast, non-complementary DNA (non-cDNA) was not able hybridize with either P2 or P3. To study the duplex DNA response to the stimuli, ATP, we then further added the formed duplex with different concentration of ATP. Figure S6b shows that in the presence of ATP, the ATP aptamer was detached from the D2, resulting with the overall dissociation of the duplex structure. This was evidenced from the electrophoresis gel result (Figure S6b) that showed the decrease in the overall duplex intensity (Green arrow) in concomitant with the increase of ATP aptamer being introduced in the system. We also detected increase intensity of 2 bands that correspond to the P2 and P3, further supporting the dissociation of D2 in response to the ATP.

FIGURE S7

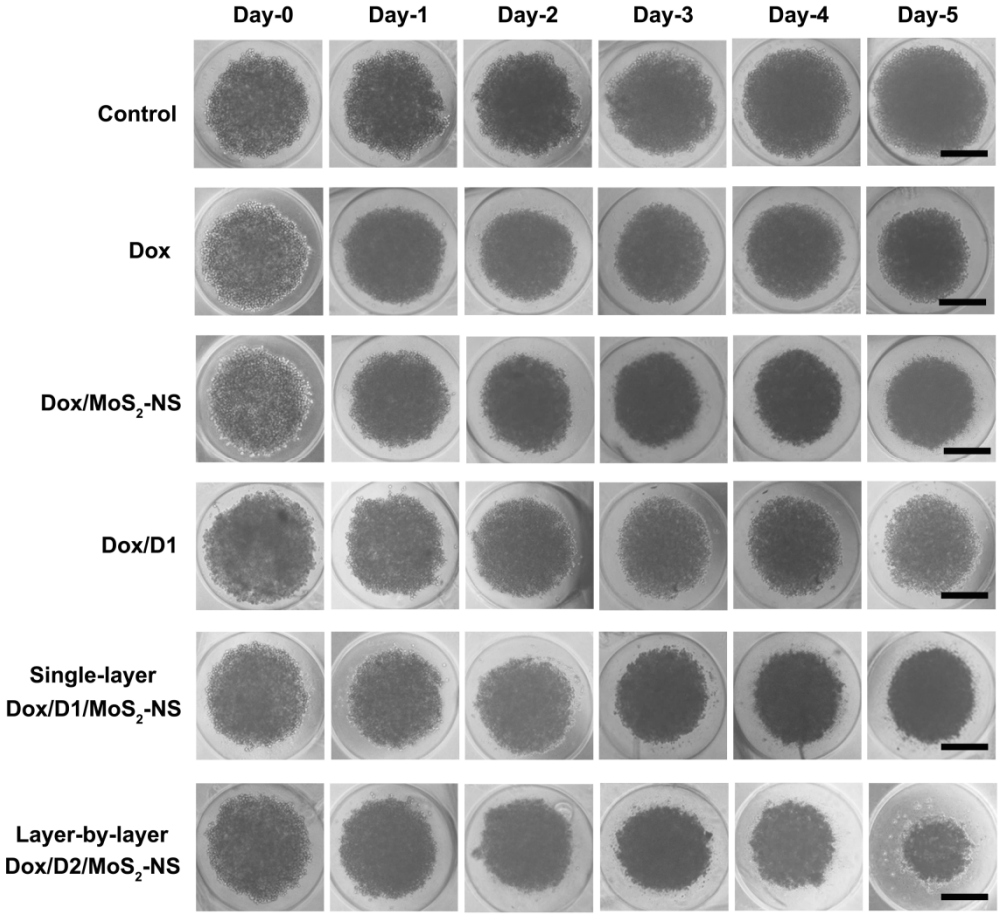

Figure S7. Phase contrast image depicts the reduction in the tumor size following sub-chronic exposure of different Dox-composites on 3D tumor spheroids over the course of 5 days treatment. Scale bar: 50 μm.

References

S1 Li, B. L.; Zou, H. L.; Lu, L.; Yang, Y.; Lei, J. L.; Luo, H. Q.; Li, N. B. Size-Dependent Optical Absorption of Layered MoS_2 and DNA Oligonucleotides Induced Dispersion Behavior for Label-Free Detection of Single-Nucleotide Polymorphism. *Adv. Funct. Mater.* **2015**, *25*, 3541-3550.

S2 Chia, S. L.; Tay, C. Y.; Setyawati, M. I.; Leong, D. T. Biomimicry 3D Gastrointestinal Spheroid Platform for the Assessment of Toxicity and Inflammatory Effects of Zinc Oxide Nanoparticles. *Small* **2015**, *11*, 702-712.

S3 Schneider, C. A.; Rasband, W. S.; Eliceiri, K. W. NIH Image to ImageJ: 25 Years of Image Analysis. *Nat. Methods* **2012**, *9*,671-675.

S4 Mo, R.; Jiang, T.; DiSanto, R.; Tai, W.; Gu, Z. ATP-Triggered Anticancer Drug Delivery. *Nat. Commun.* **2014**, *5*, 3364.

S5 Kim, D.; Jeong, Y. Y.; Jon, S. A Drug-Loaded Aptamer-Gold Nanoparticle Bioconjugate for Combined CT Imaging and Therapy of Prostate Cancer. *ACS Nano* **2010**, *4*, 3689-3696.